Proceedings of the 7th International Symposium on Cavitation
CAV2009
August 17-22, 2009, Ann Arbor, Michigan, USA

CAV2009 – Paper No. 129

Imaging the effect of acoustically induced cavitation bubbles on the generation of shear-waves by ultrasonic radiation force

Jérôme GATEAU, Mathieu PERNOT, Mickaël TANTER, Mathias FINK
Institut Langevin
ESPCI - CNRS-UMR 7587 - UNIV. PARIS 7 – INSERM ERL U979
Paris, France

ABSTRACT

In soft solids, the acoustic radiation force on bubbles generates a shear wave. This bubble-based shear wave can be imaged using high frame rate ultrasound imaging. We report here an experiment where cavitation is induced in a tissue mimicking material by an ultrasonic tone-burst excitation, which also pushes the bubbles. The generated shear wave was imaged and the energy backscattered by the bubbles measured. The tone burst excitation was iterated at the same location and the decrease of both the amplitude of the particle velocity induced by the shear wave and the backscattered energy was shown. Data treatment to extract the bubbles' contribution to this two quantities, and a simple theoretical model allowed us to point out their linear dependence.

INTRODUCTION

In soft solids, such as biological tissue or tissue phantom materials, the acoustic radiation force [1] can be generated by a momentum transfer from the ultrasonic wave to the medium through three main mechanisms. First, taking advantage of the medium viscosity, absorption-based radiation force is naturally induced by an ultrasonic beam on its path [2]. The second mechanism is related to the nonlinear propagation of ultrasonic beams leading to a zero frequency component of the signal. In medical ultrasound, such nonlinear effect of the radiation force is usually neglected. The third mechanism involves the wave reflexion on heterogeneous particles. Gas bubbles in aqueous soft solids behave as reflectors, and therefore generate a bubble-based radiation force [3] when sonicated by an ultrasonic beam.

The first mechanism induces a body force, which force density is given by [4]:

$$f_{absorption} = \alpha . \frac{2.\mathrm{I}}{c} \qquad (1)$$

where I is the local acoustic intensity, c the sound speed in the aqueous soft solid and α the ultrasound absorption coefficient of the medium. In biological tissue: $\alpha \approx 8 \;\; N_p . MHz^{-1} . m^{-1}$.

The third mechanisms generates a surface force. Its theoretical expression for a single bubble regarded as a perfect reflector is:

$$F_{bubble} = A . \frac{2.\mathrm{I}}{c} \qquad (2)$$

where A is the cross-sectional area of the bubble [3].

If we quantify the radiation force on a spherical bulk volume of tissue which has in order of magnitude the size of a cavitation bubble - i.e. a radius of R_0~10-100µm- , it comes out that, in the megahertz range, the radiation force due to absorption is about 3 orders of magnitude lower than if the volume were a bubble (cross-sectional area: $A = \pi . R_0^2$). The third mechanism is then much more efficient.

As soft solids are viscoelastic, the local displacement of the medium due to the radiation force generates a shear wave, which mainly propagates perpendicularly to the force. The speed of the shear waves c_s in soft tissues and phantom materials is typically a few meters per second, whereas the compressional wave velocity c_p , due to the high water proportion, is close to the one of water $c_p \approx 1500 \;\; m.s^{-1}$. Thanks to the large difference between these two wave velocities, the movie of the shear wave

propagation can be obtained using high frame rate ultrasound imaging [5]. c_s , which can be evaluated using the movie, is moreover directly linked to viscoelastic properties of the medium, and can then be used to estimate these properties [2]. If the medium is assumed to be purely elastic: $E \approx 3.\rho.c_s^2$ where ρ is the density and E the Young's modulus of the soft tissues.

The absorption-based radiation force has been extensively investigated, whereas the bubble-based radiation force in soft solids has only been studied experimentally (to our knowledge) by Erpelding *et al* [3]. In their studies, a bubble was induced in a homogeneous non-scattering medium (using laser-induced optical breakdown) and the radiation force was next applied on it. They were able to ultrasonically image the displacement of the bubble, which was the only scatterer available in the medium. However, the generated shear wave could not be imaged since scatterers on the propagation path are then required. On the contrary, in high scattering medium (speckle environment), it is not possible to image the bubble displacement properly because its signal is covered by the speckle noise. However, the shear waves generated by the radiation force can be imaged. We propose here to study images of shear waves generated, in highly scattering media, using cavitation bubbles.

EXPERIMENTAL SET UP

The experimental set up (Fig 1.) is based on an ultrasound probe made of a standard ultrasound imaging linear array (L7-4, 4.0/7.0 MHz Linear Array Vascular, Phillips), embedded in the center of a focused high-power single element piezoelectric transducer (2.25MHz central frequency, focal distance 70mm, *f*/# = 1, Imasonic, France) .The single element was driven by a arbitrary generator (Tektronix AFG 3101), with an RF amplifier (Amplifier research, model 75A250). For the imaging probe, the ultrasound system used was an ultrasound scanner prototype V1 developed by the company SuperSonic Imagine (Aix en Provence, France). This system is programmable per channel both in receive (64 channels) and in transmit (128 channels). Complex transmit-receive sequences enable us to image the area of the focal zone of the single element at frame rate of 2390 images/s. Basically, the ultrafast frame rate is achieved by reducing the emitting mode to a single, plane-wave insonification. All backscattered radio frequency (RF) echoes are recorded and stored into memories. The beamforming process is done only in the receive mode during a post-acquisition process.

In vitro experiments were performed in a degassed tissue mimicking phantom made of 5% gelatin gel and 3% agar powder acting as scatterers for the ultrasonic waves. The gel was prepared as follows. First, gelatin powder was melted into stirred hot (~60°C) tap water, until a homogeneous and clear gelatin solution was obtained. Agar powder was then added, and the whole solution degassed for a few minutes to avoid the introduction of air bubbles in the final gel. It was next poured into a cylindrical mould (80mm inner diameter, and 180 mm height), and the top end of the mould was sealed off with a rubber seal lid. Gelation occurred at room temperature and the gel was stored overnight at the same temperature, so that no temperature change would destabilize cavitation nuclei once the mould is opened and the gel removed to start testing.

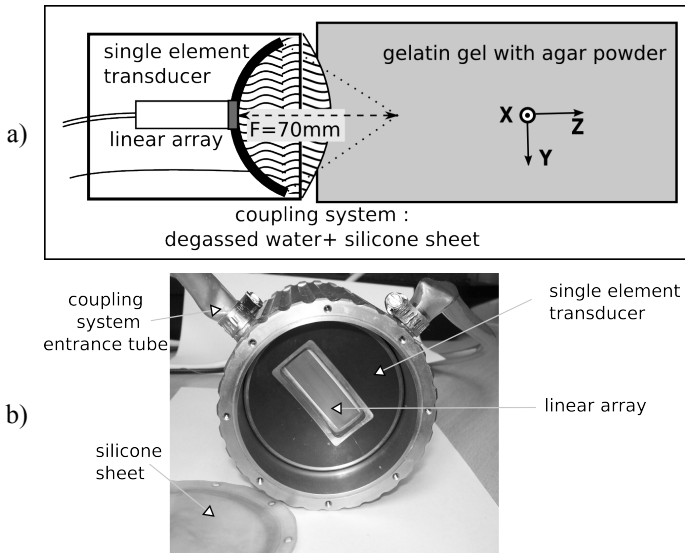

Figure 1: Experimental set-up. a) global drawing and b) picture of the ultrasonic probe

The ultrasonic imaging probe is used to transmit plane-waves (1 cycle pulse at 5MHz) at a pulse frequency repetition of 2390 Hz. A total of 26 images is achieved for the complete sequence (Fig. 2). Synchronized with this timeline, the HIFU transducer is used to probe the medium with low power pulse (3 cycles at 2.25MHz, acoustic power ~3W) and finally to generate a shear wave using high power long sonication (1000-cycles tone burst, acoustic power of ~25W).

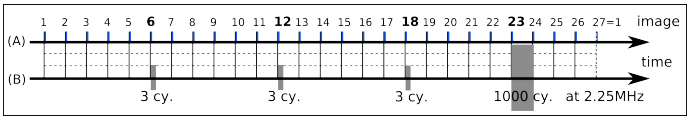

Figure 2: Basic event sequences on the linear array (A) and the single element (B). This basic sequences are repeated 11 times in a row.

For each image, the data recorded are the acoustic signals backscattered by the medium from the plane-wave transmit. Signals recorded for images n°6, 12 and 18, are also issued from the backscattering of the probing pulse. Two kind of treatment were performed on these data so as to image of the shear wave and measure the acoustic energy backscattered by the probing pulse :

- To create images of the shear wave, the velocity of the speckle motion between two successive images is computed using classic cross-correlation technique on the beamformed RF signals [6]. Shear waves are transverse waves and their direction of propagation is here perpendicular to the axis of the single-element transducer. The induced scatterers' displacement

are then mainly perpendicular to the imaging array. The obtained images are filtered spatially.

- Signals issued from the probing pulses are extracted by subtracting the RF data from the previous image, the time interval corresponding to the focal spot is selected, and the acoustic energy is integrated over this time interval (~30µs). This computed result is denoted E_{ac} .

RESULTS

Data were recorded for 11 iterations of the sequences in a row, which corresponds to ten successive generations of shear wave at the same spot.

Images of the particle velocity field induced by the first iteration of the sequences, at different time instants of its propagation, are shown on Fig. 3 . All images have the same color scale. The coordinate (x,z)=(0,70mm) corresponds to the focal point of the single-element transducer.

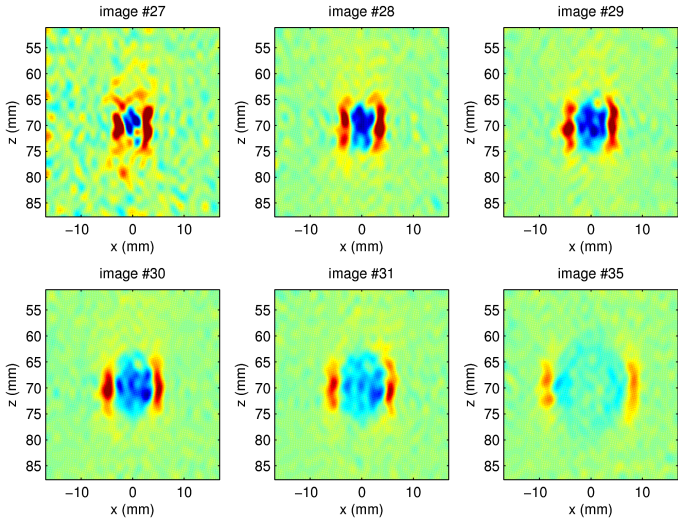

Figure 3: Experimental movie of particle velocities on the first five images (images number 27 to 31) plus the 9th one (image number 35) of the 2nd sequence.

The 1000-cycles tone-burst excitation of the medium does generate a shear wave (Fig. 3.). This wave is propagative and has a cylindrical shape. Due to spreading loss, the particle velocity decreases as the wave propagates away from its source, that is to say the focal spot of the single element.

Fig. 4. presents stroboscopic images of the first four shear waves, obtained ~3ms after the tone-burst. All images have the same color scale.

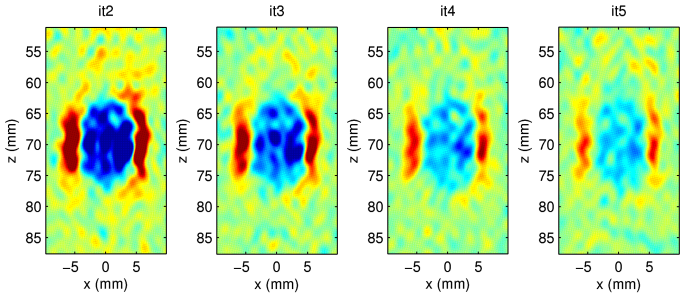

Figure 4: Particle velocity field induced by the shear wave on the 5th image of the sequence, for the 2nd to the 5th iteration.

The amplitude of the particle velocity field induced by the shear wave decreases as the sequences are iterated. However, the global shape of the wave (spatial velocity distribution) stays the same. The evolution of the particle velocity distribution over the iterations is shown on Fig. 5 for the z-coordinate of the focal plan of the single-element transducer (z=70mm).

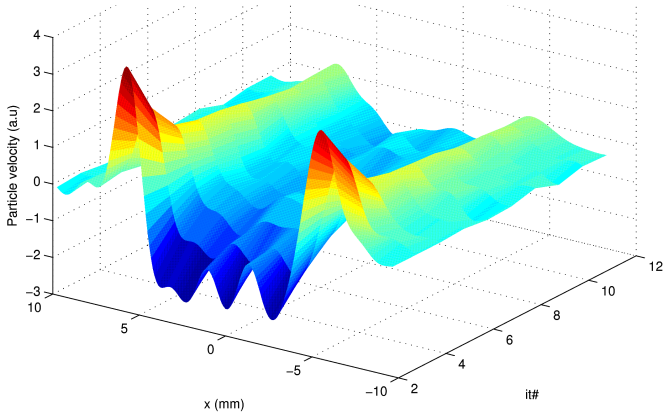

Figure 5: Particle velocity field induced by the shear wave on the 5th image of the sequence plotted here for the points located at the z-coordinate: z=70mm, and for all the successive iterations.

Fig 6. combines the plots of two main sets of data versus the iteration number. The first main set is composed of three sub-sets marked with triangles which correspond to the values of E_{ac} computed respectively from the images 6, 12 and 18 over the iterations. The second main set corresponds to the amplitude of the shear wave on the image 5. This amplitude is measured by the maximum particle velocity in the focal plane of the single element for the right part of the shear wave (x>0). For easy comparison, its minimum was subtracted from each main data set and data were normalized.

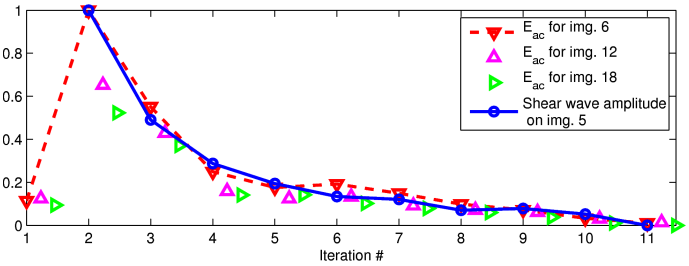

Figure 6: Extra acoustic energy and shear wave amplitude versus the sequences iteration

THEORETICAL MODEL

We present here a simple theoretical model to link the particle velocity induced by the shear wave to the backscattered acoustic energy, when both are due to the presence of cavitation bubbles. The above experiment defines the framework of the model.

The acoustic radiation force on a single bubble is usually considered to be caused by a pressure gradient $\vec{\nabla} P$ and body volume V oscillations. The resulting force is then given by :

$$\vec{F} = -\langle V . \vec{\nabla} P \rangle \tag{4}$$

where < > indicates time average.

Considering a sinusoidal propagative acoustic plane wave driving the bubble, this force is given by the following equation [7 p. 343-344] :

$$F_g = \frac{2.\pi.R_0.I}{\omega} . \frac{2.\beta_{tot}/\omega}{((\omega_0/\omega - 1)^2 - 1)^2 + (2.\beta_{tot}/\omega)^2} \tag{5}$$

where ω is the pulsation of the incident wave, I its average acoustic intensity. ω_0 is the resonance pulsation of the bubble, R_0 its equilibrium radius, β_{tot} the total resistive constant leading to damping.

For bubbles significantly larger than the resonance size ($\omega \gg \omega_0$), this radiation force vanishes and an other approach has to be considered. A gas body in an aqueous soft solid is a perfect reflector, and indeed leads to a radiation force given by:

$$F_r = \frac{2.I.A}{c_p} \tag{6}$$

where c_p is the compressional wave velocity in the soft solid and A the cross-sectional area of the bubble [3].

Moreover, the prefect reflection condition gives:

$$I.A = E_{ac}^A \tag{7}$$

where E_{ac}^A is the acoustic energy backscattered by the bubble.

For a single bubble driven far above the resonance, the radiation force, which applies on it, is then given by :

$$F^A = \frac{2}{c} . E_{ac}^A \tag{8}$$

For our study, a bubble cloud is more likely to be formed than a single bubble from the high power insonication of the medium. To model this multi-bubble situation, two main assumptions are made. First, we assume that the cavitation nuclei growth occurs fast enough to be able to consider that most of the bubbles excess the resonance size (about a few microns in order magnitude at 2.25MHz) for most of the duration of the tone burst. Secondly, the bubbles are supposed to be independent (no interaction between them, and no multi-scattering).

The number of bubbles per unit volume with cross-sectional area between A and A +dA is noted $n_A . dA$. The body radiation force density created at the location $\vec{\xi}$ in the bubble cloud can then be express as:

$$f(\vec{\xi}) = \frac{2}{c} . \int_A n_A(\vec{\xi}) . E_{ac}^A . dA = \frac{2}{c} . e_{ac}(\vec{\xi}) \tag{9}$$

where $e_{ac}(\vec{\xi})$ is the backscattered energy density.

Heterogeneous cavitation is a random phenomena depending both on the nuclei spacial and size distributions. For the simplicity of the model, we then assume that the distribution of the bubbles is constant over the tone-burst duration and that the relative size distribution on each position stays the same for each iteration of the sequences. However, as the medium is static, each tone burst causes nuclei depletion and as a result the amplitude of quantity $n_A(\vec{\xi})$ decreases sequence after sequence. This decrease is assumed to be the same for every position. The radiation force distribution for the iteration number "i" is then given by:

$$\forall \vec{\xi}, \quad f^{\#i}(\vec{\xi}) = a_i . f^{\#1}(\vec{\xi}) \qquad (a_i \le 1) \tag{10}$$

and as a consequence:

$$\forall \vec{\xi}, \quad e_{ac}^{\#i}(\vec{\xi}) = a_i . e_{ac}^{\#1}(\vec{\xi}) \qquad (a_i \le 1) \tag{11}$$

The acoustic energy backscattered by the bubbles located in the focal spot of the single element is then for the interaction number "i" :

$$E_{ac}^{\#i} = \iiint_{V_{\text{foc spot}}} e_{ac}^{\#i}(\vec{\xi}) . d\vec{\xi} = a_i . E_{ac}^{\#1} \tag{12}$$

The particle velocity field induced by a source distribution $\vec{f}(\vec{\xi}, t)$ in a viscoelastic medium can be deduced from the elastic Green's function $\vec{g}_v(\vec{r}, t)$ by [8] :

$$\vec{v}(\vec{r},t)=\int_{\tau} d\tau \iiint_{V} \vec{f}(\vec{\xi},\tau).\vec{g}_v(\vec{r}-\vec{\xi},t-\tau).d\vec{\xi} \quad (13)$$

As the force distribution is assumed to be constant during the tone burst:

$$\vec{v}^{\#i}=\int_{\text{Tone burst \#i}} d\tau \iiint_{V_{\text{foc spot}}} \vec{f}^{\#i}(\vec{\xi}).\vec{g}_v(\vec{r}-\vec{\xi},t-\tau).d\vec{\xi}$$

$$\vec{v}^{\#i}=a_i.\int_{\text{Tone burst \#1}} d\tau \iiint_{V_{\text{foc spot}}} \vec{f}^{\#1}(\vec{\xi}).\vec{g}_v(\vec{r}-\vec{\xi},t-\tau).d\vec{\xi}$$

where $V_{\text{foc spot}}$ is the volume of the focal spot and $0\le t\le T$ where T is the duration of one sequence.

It comes out that :

$$\vec{v}^{\#i}(\vec{r},t)=a_i.\vec{v}^{\#1}(\vec{r},t) \quad (0\le t\le T) \qquad (14)$$

From equation (12) and equation (14), we deduce that the contribution of the bubble to the particle velocity field and the backscattered energy can be linked by:

$$\frac{\left\|\vec{v}^{\#i}\right\|}{\left\|\vec{v}^{\#1}\right\|}=\frac{E_{ac}^{\#i}}{E_{ac}^{\#1}} \qquad (15)$$

where ||.|| indicates the Euclidean norm of a vector.

According to equation (15), the amplitude of the particle velocity field induced by the shear wave depends linear on the bubble density, like the backscattered energy.

This model is very simple and ignores the complex aspects of the bubble population phenomena that occurs in acoustic cavitation, nevertheless it gives clues to understand the basic physic at stake in the experiment.

DISCUSSION

The results presented on figure 6 are repeatable and show some interesting phenomena: the acoustic energy E_{ac} backscattered by the focal spot of the single element was low for the first iteration, and raised dramatically just after the first tone-burst, to decrease again for the next iterations following the same decreasing pattern as the shear wave amplitude. These phenomena are interpreted as follows: the cavitation nuclei in the focal area of the single element are destabilized by the first tone-burst and the induced bubbles both contribute to the radiation force and strongly backscatter the following probing pulses. Then, as the medium is static and the pushes are repeated every ~11ms, the bubble and nuclei population decreases by dissolution or fragmentation (successive excitation of the medium) in the insonified area. Consequently, both the acoustic energy E_{ac} and the radiation force decrease until only gel natural scatterers (agar powder) and absorption play a role for these two quantities respectively. Thus, subtracting its minimum from each main data set, for figure 6, enabled us to extract the bubbles' contributions.

The energy backscattered from the tone-burst transmit could not be recorded properly because it saturated the detector. But as there are only 3 ms between the end of the tone-burst and the first probing pulse, we assume that the bubble population has not evolved much and that the backscattered acoustic energy recorded reflects the bubble population available during the shear wave generation. Then, our simple theoretical model is able to explain the linear dependence between the amplitude of the shear wave and the energy backscattered from the first probing pulse.

Further experiments have been carried out to separate the bubble generation from the shear wave generation. The aim was to better understand the phenomena at stake in this complex system. Such experiments imply that the acoustic signal which induces cavitation (ideally a high power short pulse so as not to generate significant motion) and the acoustic signal that pushes the bubble can be distinguished. We tried different experimental set-ups to be able to modify the amplitude ratio between these two signals, their length and their frequency (since the cavitation threshold is higher at high frequency) but heterogeneous cavitation in tissue phantom materials is difficult to control and more time would be needed to get valuable results.

CONCLUSION

A close relationship has been found between the cavitation bubble population and the amplitude of the shear wave generated by radiation force on this population.

As the shear wave amplitude depends directly on the presence and the number of cavitation bubbles or their nuclei, shear wave imaging could be used to detect cavitation in highly scattering medium. Optical detection can be considered too [9]. Moreover, other properties of the shear wave such as the shape and spectrum may also be linked to the cavitation properties.

ACKNOWLEDGMENTS

The authors would like to thank Emmanuel BOSSY for helpful discussions.

REFERENCES

[1] Chu T. , R. E. Apfel 1982, “Acoustic radiation pressure produced by a beam of sound, ” *J. Acoust. Soc. Am.*, 72,. 1673-1687.

[2] Sarvazyan A. P., Rudenko O. V., Swanson S. D., Fowlkes J. B., Emelianov S. Y. 1998, “Shear wave elasticity imaging: A new ultrasonic technology of medical diagnostics,” *Ultrasound Med. Biol.*, 24 (9), 1419–1435.

[3] Erpelding, T.N., Hollman, K.W., O'Donnell, M. 2005, “Bubble-based acoustic radiation force elasticity imaging” *UFFC IEEE Transactions,* 52 (6), 971-979

[4] Torr G.R., 1984, “The acoustic radiation force” *American Journal of Physics,*52, 402-408

[5] Bercoff, J., Tanter, M., Fink, M. 2004, “Supersonic shear imaging: a new technique for soft tissue elasticity mapping” *UFFC IEEE Transactions,*51 (4), 396-409

[6] Bonnefous, O., Pesque, P. 1986, “Time domain formulation of pulse-Doppler ultrasound and blood velocity estimation by cross correlation” *Ultrason Imaging*, 8 (2), 73-85.

[7] Leighton T.G., 1994, “The Acoustic Bubble” *Academic Press*

[8] Bercoff, J., Tanter, M., Muller, M., Fink, M., 2004, “The role of viscosity in the Impulse Diffraction Fiels of Elastic Waves Induced by the acoustic Radiation force” *UFFC IEEE Transactions,* 51 (11), 1523 - 1536

[9] Bossy E., Funke A. R., Daoudi K., Boccara A. C., Tanter M., Fink M. 2007, “Transient optoelastography in optically diffusive media” *Appl. Phys. Lett.* 90, 174111